A case study on the matrix approach to WEC performance characterization

Conference Paper · September 2015

CITATIONS
3

READS
2,107

4 authors:

Clayton E. Hiles
Kerr-Wood-Leidal Consulting Engineers
17 PUBLICATIONS **319** CITATIONS
SEE PROFILE

Adrian David de Andres
The University of Edinburgh
30 PUBLICATIONS **675** CITATIONS
SEE PROFILE

Scott J. Beatty
MarineLabs Data Systems Inc.
20 PUBLICATIONS **555** CITATIONS
SEE PROFILE

B. Buckham
University of Victoria
120 PUBLICATIONS **2,989** CITATIONS
SEE PROFILE

A case study on the matrix approach to WEC performance characterization

Clayton Hiles*, Adrian David De Andres Guitierrez†, Scott Beatty‡ Brad Buckham‡
*Cascadia Coast Research Ltd.
Victoria, BC, Canada
E-mail: clayton@cascadiacoast.com
†Institute of Energy Systems,University of Edinburgh
Edinburgh, Scotland
E-mail: adrian.deandres@ed.ac.uk
‡West Coast Wave Initiative, University of Victoria
Victoria BC, Canada
E-mail: scottb@uvic.ca; bbuckham@uvic.ca

***Abstract*—The influence of the dimensionality of the performance matrix and the duration of the performance data series on the power performance assessments by the IEC/TS-62600-100 and IEC/TS-62600-102 specified methodologies are assessed using time-domain model simulations of wave energy converter. The wave energy converter is a two-body self-reacting point absorber with an optimum passive damping power take-off. A 3D performance matrix approach, where the additional dimension is spectral bandwidth, is shown to improve the accuracy of mean annual energy production calculations. In the IEC/TS-62600-100 analysis, the 3D approach reduces error 2-3% and in the IEC/TS-62600-102 analysis, the 3D approach reduces error 10-15% The duration of the performance data series is shown to be more critical for the IEC/TS-62600-100 analysis; However, the criticality is reduced when a 3D performance matrix is used. Lastly, the duration of the performance data series is shown to be less critical for the IEC/TS-62600-102 analysis.**

***Index Terms*—Wave energy conversion, power performance matrix, uncertainty, variability, standards, sensitivity to spectral shape**

I. Introduction

Wave energy conversion is still in the prototype testing stage and several prototypes with different principles are still being considered. When analysing the market perspectives for a particular Wave Energy Converter(WEC), the computation of the prospective Levelized Cost of Energy is an important parameter to take into account. In the calculation of this parameter, the energy production of the converter during its life-cycle, is a key element.

The working groups PT100 and PT102 of the TC114 are tasked with generating equitable and standardized methods for evaluating and characterizing the performance of WEC technologies. IEC/TS-62600-100ed1.0 was published by PT100 in 2012 [1]. This specification provides guidance on power performance assessment at a single site based on a specified set of measurements. IEC/TS-62600-102 is currently being drafted by PT102. This specification will provide guidance on how to estimate WEC performance at a second location based on an IEC/TS-62600-100 type analysis.

The basic method used by both the PT100 and PT102 is the performance matrix approach. In this approach the WEC power performance is characterized over discrete range of met-ocean data using the method of bins. Traditionally the wave parameters *significant wave height* and *energy period* are used to create an easily conceptualized two-dimensional performance matrix. However, the approach may be extended into an arbitrary number of dimensions. Once constructed, the performance matrix is then interpolated using a long term met-ocean data-set to a yield a long-term estimate of performance. This record may then be appropriately averaged to determine the mean annual energy production (MAEP).

One issue currently under investigation within the TC114 is the appropriate dimensionality of the performance matrix. For many WECs under development, characteristic wave height and period are insufficient to describe the variability of WEC performance. For example, a bottom mounted pitching flap type device may be sensitive to wave direction, while a self reacting point absorber may be sensitive to spectral shape. Failing to account for these parameters in the performance matrix approach can lead to large errors in performance estimates.

A second issue that warrants investigation is the length of the data-set needed to generate a performance matrix which yields accurate MAEP estimates at Location 1. Currently IEC/TS-62600-100ed1.0 recommends a minimum of six months of performance measurements, however there is no clear basis for this recommendation.

II. Literature Review

When calculating the performance of a device on a second location, the variability of the met-ocean conditions is a very important issue to take into account. However, traditionally only two spectral parameters are used (H_{m0} and T_e) for power characterization. Kerbiriou et al., in [2] and [3], studied how an improved characterization of sea states influences the performance of a WEC. They stated that analytical spectra

produce power estimates erroneous by 63% due to the existence of sea states with more than one peak. They concluded that the sea state characterization with analytical spectra could cause large errors in power production estimates. In the case of the SEAREV device located at the SEMREV test site, they concluded that the analytical spectrum led to an underestimation of the harvested power by the device.

Saulnier et al. [4] studied the sensitivity of the wave groupiness and spectral width for some wave energy converters. They concluded that the sensitivity of a WEC to spectral width is more significant when the mean period is near the resonance period of the device and also when the response of the WEC is broad. Saulnier et al. [5] studied the distribution of the different sea states that occur on the Portuguese coast in terms of the number of modes and directionality. The literature demonstrates that the sea state characterization significantly influences the numerically calculated power performance of a converter. Thus, it is clear that sea state characterization estimates influence long term power performance estimates and an accurate approach is needed to estimate the MAEP for WECs.

This issue was also investigated for an specific device (Oscillating Wave Surge Converter) by [6]. They concluded that the performance of the OWSC is more sensitive to spectral energy distribution in short period seas. This is explained by the consistency of power capture from lower frequency spectral components and the decline in power capture from higher frequency spectral components. Furthermore they concluded that, for all seas, the power captured by the OWSC decreases as the seas spectral bandwidth increases. This is explained by the increased proportion of sub-optimally damped spectral components in seas of wider spectral bandwidth.

Pascal et al [7] experimentally investigated the influence of a range of sea state parameters on the performance of three types of WECs with different directionality characteristics. They concluded that there is no evidence that only T_e and H_{m0} should be retained for the performance estimation of wave energy devices. Lastly, in [8] and [9] the classical method of power production assessment was found to be very inaccurate in those areas with high percentage of multimodal spectra (combined SEA and SWELL sea states). In this case, the use of more spectral parameters apart from the H_{m0} and the T_e is highly recommended in order to avoid large errors. As it has been demonstrated, there are several studies that question the suitability of the 2D (H_{m0},T_e) performance matrix. However there are no studies that investigate the influence of the length of the WEC performance data series on the quality of the power assessment.

In this work, a time-domain model ([8], [10]) of a two-body self-reacting point absorber—a WEC configuration known to be sensitive to spectral shape—is used to investigate the influence of: the dimensionality of the performance matrix, and the length of the met-ocean data series, on the power performance under the IEC/TS-62600-100 and IEC/TS-62600-102 specifications. The analyses are carried out in four major steps:

1) the time domain model is used to calculate the hourly power performance the WEC operating at a reference location (called Location 1: La Perouse Bank, BC, Canada) and at a second deployment location (Location 2: Osbourn Head, NS, Canada)
2) IEC/TS-62600-100 and IEC/TS-62600-102 methodologies are applied to calculate the MAEP at both Location 1 and Location 2.
3) The effect of introducing spectral bandwidth as an additional dimension to the performance matrix on the accuracy of the calculated MAEP is assessed.
4) The effect of data record duration on the accuracy of the calculated MAEP is assessed.

III. Methods

A. Site Selection

Location 1 was selected to correspond to the site of Environment Canada wave measurement buoy c46206 at La Perouse Bank, on the Pacific Coast of Canada. This buoy is about 30 km offshore from the communities of Tofino and Ucluelet, BC. Over the past 15+ years there has been a sustained interest in developing wave energy in this region which has recently coalesced with the formation and funding of the West Coast Wave Initiative at the University of Victoria[1].

Location 2 was selected to correspond to Marine Environmental Data Service buoy meds103 at Osbourne Head, on the Atlantic Coast of Canada. This buoy is about 6 km offshore and about 15km from the City of Halifax, NS. Location 2 was selected as a plausible region of wave energy development with spectral characteristics of the wave climate which are distinctly difference from Location 1.

Characteristics of the wave climate at each location will be discussed in the following section.

B. Wave Data Analysis

Wave data from both locations was obtained from the Department of Fisheries and Oceans Canada as one dimensional variance density spectra, ($S(f)$), [11]. From the variance density spectra the significant wave height (H_{m0}), energy period (T_e) and spectral width (ϵ_0) were calculated as in the following equations:

$$H_{m0} = 4\sqrt{m_0} \tag{1}$$

$$T_e = m_{-1}/m_0 \tag{2}$$

$$\epsilon_0 = \sqrt{m_0 m_2/m_1^2 - 1} \tag{3}$$

where the n$^{\text{th}}$ spectral moment, m_n, is given by:

$$m_n = \sum f^n S(f) df \tag{4}$$

and where f is the bin-centre frequency and df is the frequency bin-width.

Additionally the spectra were analysed using the methods of [12] to identify the number of swell and sea modes.

[1] http://www.uvic.ca/research/projects/wcwi/

TABLE I
DATA AVAILABILITY, QUALITY AND CHARACTER FROM BUOYS *c46206* AND *meds037*

	Location 1 La Perouse Bank, BC	**Location 2** Osbourn Bank, NS
Buoy ID	c46206	meds037
Lat	48.8350	44.5219
Lon	125.9980	63.4230
Depth	72 m	57 m
Sample Interval	1 hr	1 hr
Years Used	2001-2013	1988-2001
# Total Records	96131	177424
# Good Records	85741	171510
H_{m0} (10%ile)	0.97 m	0.50 m
H_{m0} (50%ile)	1.94 m	1.07 m
H_{m0} (90%ile)	3.68 m	2.51 m
T_e (10%ile)	6.9 s	6.7 s
T_e (50%ile)	8.8 s	8.2 s
T_e (90%ile)	11.1 s	9.9 s
ϵ_0 (10%ile)	0.38	0.18
ϵ_0 (50%ile)	0.46	0.23
ϵ_0 (90%ile)	0.58	0.34

Included in the wave data is a quality code indicator [11]. Only wave data indicated with a *good* quality code was used. A summary of the data availability, quality and character from each of the buoys is provided in Table I.

The wave climate in the region of Location 1 on the Pacific is characterized by energetic winters and much calmer summers. During the winter, swell is typically generated by large storms in the North Pacific and arrives from the north-westerly direction, though, significant wave systems can also be generated more locally by high winter winds. During the summer waves are typically generated by low magnitude local winds. In addition, during the summer there is often a long period swell arriving from the south. This swell originates in winter storms in the Southern Ocean. As a result of this southern swell contribution, wave spectra in the summer are often double peaked. The spectral width is relatively constant throughout the year with a range of about 0.3-0.5 and a mean value of 0.4.

The wave climate at Location 2 on the Atlantic is characterized again by energetic winters and calmer summers. However, there is significantly more day-to-day variability in the wave height at Location 2 compared to Location 1. Large waves are generated by local storms that quickly give way to calm conditions. The sea-states occurring at Location 2 are characterized primarily as wind seas and often contain more than one peak. The spectral width is typically narrower than Location 1. In the winter ϵ_0 ranges from 0.2 to 0.5 with a mean of about 0.28. In the summer ϵ_0 is typically smaller with a range of 0.2 to 0.35 and a mean value of 0.25.

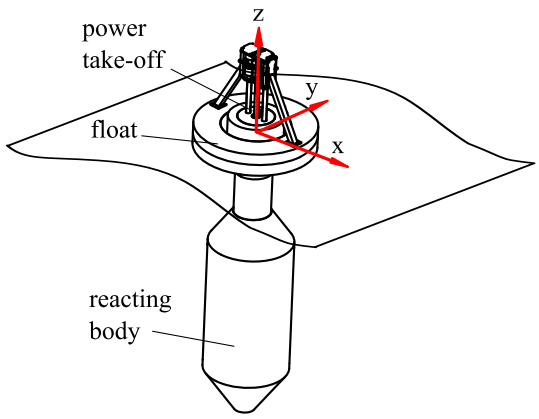

Fig. 1. Schematic of the WEC configuration

TABLE II
SUMMARY SPECIFICATIONS OF THE WEC

Parameter	Value	Units
Draft	35	m
Float Displacement	201	tonnes
Reacting Body Displacement	1644	tonnes
Float outer diameter	14.75	m

C. WEC Specifications

The WEC device used to undertake this study is a two-body self-reacting point absorber modeled after a WaveBob^{TM}(WaveBob Ltd., Ireland), as shown in Figure 1. The WEC operates primarily in heave. Forces from incident waves cause the buoyant, toroidal shaped float to react against a second body, referred to as the reacting body. The relative reaction forces do useful work through a power take-off. The power take off force is typically adjusted in order to optimize the useful work extracted. Summary specifications of the WEC are given in Table II .

D. WEC Numerical Model

The equations governing the heave dynamics of the two-body WECs are given by:

$$(\boldsymbol{M} + \boldsymbol{A}(\infty))\ddot{\vec{\xi}}(t) = \boldsymbol{F}_e(t) + \boldsymbol{F}_r(t) + \boldsymbol{F}_c(t) + \boldsymbol{F}_v(t) + \boldsymbol{F}_k(t) + \boldsymbol{F}_{pto}(t) \quad (5)$$

where heave displacement, velocity, and acceleration of the float and reacting body are represented respectively by 2x1 vectors: $\vec{\xi}$, $\dot{\vec{\xi}}$, and $\ddot{\vec{\xi}}$. $\boldsymbol{M}+\boldsymbol{A}(\infty)$ is a 2x2 mass matrix combined with the infinite frequency added mass. The remaining terms are 2x1 vectors, where $\boldsymbol{F}_e$ are excitation forces, $\boldsymbol{F}_r$ are radiation forces, $\boldsymbol{F}_c$ are Coulomb friction forces, $\boldsymbol{F}_v$ are viscous drag forces, $\boldsymbol{F}_k$ are hydrostatic forces, and finally $\boldsymbol{F}_{pto}$ are PTO forces. As per the Cummins approach [13], radiation and excitation forces are respectively modelled for each body j by

the following convolution integrals:

$$F_{r,j}(t) = -\int_0^\infty k_{r,j}(\tau)\dot{\xi}_j(t-\tau)d\tau \quad (6)$$

$$F_{e,j}(t) = \int_{-\infty}^\infty k_{e,j}(\tau)\eta(t-\tau)d\tau, \quad (7)$$

where the radiation and excitation kernel functions are given by:

$$k_{r,j}(t) = \frac{-2}{\pi}\int_0^\infty \omega(A_j(\omega) - A_j(\infty))sin(\omega t))d\omega \quad (8)$$

$$k_{e,j}(t) = \frac{1}{2\pi}\int_{-\infty}^\infty X_j(\omega)e^{i\omega t}d\omega \quad (9)$$

The convolution integral bounds are chosen to be wide enough so that kernel functions have approached zero in the time ranges (0 to 10 sec for radiation, -10 to 10 sec for excitation). A sliding friction force is included to account for the friction in the linear guide bearings on which the float and reacting bodies translate. The sliding friction force on body is modelled using the Coulombic model with constant force. The viscous drag force on body j is modelled using the the relative velocity formulation of the Morison drag force [14]:

$$F_{v,j}(t) = -\rho\frac{\pi}{8}D_j^2 C_{D,j}\left|\dot{\xi}_j(t) - v_j(t)\right|\left(\dot{\xi}_j(t) - v_j(t)\right) \quad (10)$$

where D_j is the characteristic diameter, $C_{D,j}$ is the drag coefficient, and v_j is taken as the fluid velocity at the depth location of the characteristic diameter. D_1 is taken as the float outer diameter and D_2 is taken as the largest diameter of the reacting body.

A 4th order Runge-Kutta, fixed time-step, integrator with a time step of 0.065 seconds is used for the time simulations. The time domain model runs at approximately 10:1 real-time.

A numerical optimization of the value was completed for each wave spectrum. The optimization problem maximizes power converted, taking the spectrum shape into account. Computed in the objective function, the WEC dynamics are calculated using a frequency domain model with experimentally determined, linearized, viscous drag terms, validated in Beatty et al [10].

E. Analysis at Location 1

WEC performance is first evaluated at Location 1 at La Perouse Bank. The objective is to assess the accuracy of the methods of IEC/TS-62600-100ed1.0 [1] in estimating the mean annual energy production (MAEP) at Location 1.

1) 'Truth Signal': To enable this assessment, the time-domain model was first used to generate a multi-year time-series of absorbed power (P_{abs}) that, in this analysis, is used as a 'truth' signal. The model was used to simulate WEC performance at Location 1 from 2001 to 2013 for each available hourly wave record. The buoy measured wave spectra were used as input conditions. Each simulation was run for 21 simulated minutes. The resulting instantaneous power time-series from each simulation were then averaged to yield a representative mean power record.

The mean annual energy production is calculated directly from the simulated mean absorbed power record:

$$MAEP = \frac{T}{n}\cdot\sum_{i=1}^{1=n} P_{abs} \quad (11)$$

Where T is the average length of a year (8766 hr), i indicates the record number and n is the total number of records in the data set.

2) Performance Matrix Approach: IEC/TS-62600-100ed1.0 specifies that the method of bins is used to generate a *performance matrix* [1]. *Capture length* is used as the performance metric, and matrix has dimensions of at minimum H_{m0}, T_e. The specification also states that additional dimensions may be added to the performance matrix to reduce the variability of the capture length values falling into each bin.

Capture length is calculated as the quotient of the electrical power output from the WEC and the incident wave energy flux. In this work, we will assume a 100% efficient power take off (PTO) system so that the electrical power is equal to the mechanical power absorbed by the WEC, and capture length (L) is calculated as:

$$L = P_{abs}/J \quad (12)$$

where J is the incident wave power flux:

$$J = \rho g\sum C_g(f)S(f)\Delta f \quad (13)$$

$C_g(f)$ is the group velocity and P_{abs} is calculated by the time-domain model. Applying (12) to the multi-year wave and WEC performance records, the result is a time-series of capture length records. The method of bins is applied to the L time-series and for each bin the mean, minimum, maximum, standard deviation and number of records is recorded.

To estimate the long term power performance of the WEC, a minimum of 10 years of met-ocean data is recommended in [1]. The met-ocean data which define the dimensions of the performance matrix (e.g. H_{m0} and T_e) are used to interpolate the mean value of L_i for each wave record. The MAEP is then estimated as:

$$MAEP = \frac{T}{n}\cdot\sum_{i=1}^{i=n} L_i\cdot J_i \quad (14)$$

F. Analysis at Location 2

WEC performance is next evaluated at Location 2 at Osbourn Head, NS. The objective is to assess the accuracy of the methods under development by the PT102 to estimate MAEP at Location 2, based on a performance data collected at Location 1.

1) 'Truth Signal': Like Section III-E, the time domain model is used to create a 'truth' signal for the WEC performance at Location 2 for the years 1998-2001.

2) Performance Matrix Approach: Following the methods proposed by the PT102, the WEC performance is estimated by interpolating the performance matrix generated for Location 1, using the met-ocean data from Location 2. While the PT102 has proposed methods for augmenting the performance matrix such as interpolation and extrapolation of undefined bins, these are not considered here.

IV. Results and Discussion

Here we examine the increase in accuracy in the performance matrix achieved by increasing the dimensions of the performance matrix from 2 (H_{m0}-T_e) to 3 (H_{m0}-T_e-ϵ_0). First, the 13 year absorbed power time-series estimated using the performance matrix approach is compared to that estimated using the 2D and 3D capture length matrices. Then, we examine how the accuracy of the MAEP changes with the duration of the data record used to calculate the performance matrices.

A. Analysis at Location 1

1) Time-series: The capture length record from the complete 13 years of time domain simulations was used to generate 2D (H_{m0}-T_e) and 3D (H_{m0}-T_e-ϵ_0) capture length matrices.

The 2D capture length matrix ($2DL$) for the full 13 year data set is given in Fig. 2, the 3D capture length matrix ($3DL$) is not shown. Where there is no data available, the bins of Fig. 2 are left blank. The occurrences of large wave height, short period waves are notable. These occurrences likely result from erroneous wave data not flagged by quality assurance process. Since we have no clear basis for rejecting these records, they have been retained.

The $2DL$ and $3DL$ were interpolated using the met-ocean data from Location 1 to estimate of the mean P_{abs} record. These records are compared to the 'truth' signal generated with the time domain model. Shown in Figs. 3 and 4 are scatter plots comparing the P_{abs} as calculated by the time domain simulation model (indicated as 'TD') with the P_{abs} estimated by interpolation of the $2DL$ and $3DL$ matrix respectively. The colours in the scatter indicate the value of ϵ_0.

Figure 3 indicates a ϵ_0 dependant bias in $2DL$ estimates of P_{abs}. For spectra with wider frequency distribution, the interpolation of the $2DL$ matrix over-estimates performance. This occurs because the device performance degrades with higher spectral width. In the $2DL$ matrix the performance variability due to ϵ_0 is not accounted for and is essentially averaged out in each bin. As a result of this averaging, interpolation of the $2DL$ tends to over-estimate P_{abs} for large ϵ_0 and under-estimate for small value of ϵ_0.

Overall the P_{abs} time-series estimated using the $2DL$ matrix is reasonable; the bias, rms error and correlation coefficient are: -0.1kW, 8.2kW, 98%.

Figure 4 does not show the same ϵ_0 dependant bias in P_{abs} estimates that is observed in is Fig. 3. The P_{abs} time-series estimated using the $3DL$ matrix is improved over that using the $2DL$. The scatter in Fig. 4 is visibly reduced and the bias, rms error and correlation coefficient are improved to -0.2kW, 6.0kW, 99%.

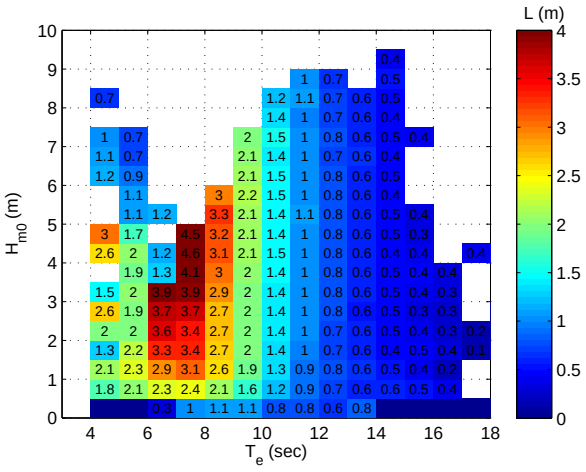

Fig. 2. 2D capture length matrix constructed from 13 years of performance simulations at Location 1.

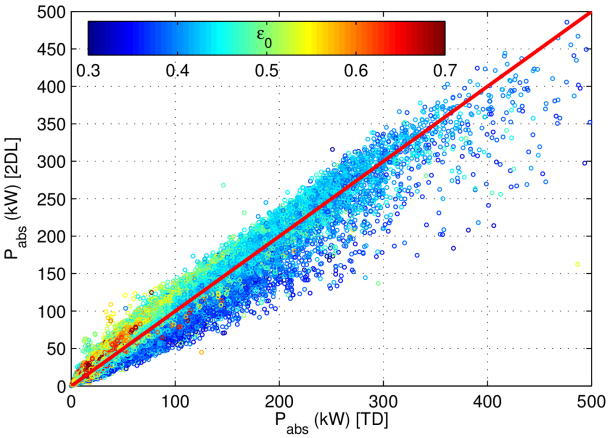

Fig. 3. Scatter plot comparing power performance estimated using the $2DL$ matrix to the 'truth' signal from the time domain model (TD) at Location 1.

2) MAEP: Here we investigate the length of the data-set needed to generate a performance matrix which yields accurate MAEP estimates at Location 1. Where Section IV-A1 used all 13 years of available performance data to produce the 2D and 3D matrices, here we repeat that procedure using 1,2,3...13 years of performance data.

Table III compares the 'true' MAEP, calculated with the time domain model, to the MAEP estimated from the $2DL$ and $3DL$ matrices, as a function of the length of the performance data set; the percentage difference is plotted in Fig. 5. The table and figure clearly show that for a short length of available data, the 3D matrix improves the MAEP estimate. With increased data both the $2DL$ and $3DL$ MAEP estimates improve and eventually converge to a similar result. The $2DL$ estimate requires about 6 years of data to converge with 1% of the 'true' MAEP, while the $3DL$ estimate requires only 2 years.

Both the $2DL$ and $3DL$ matrices yield reasonable estimates of the MAEP at Location 1, even with just 1 year of data.

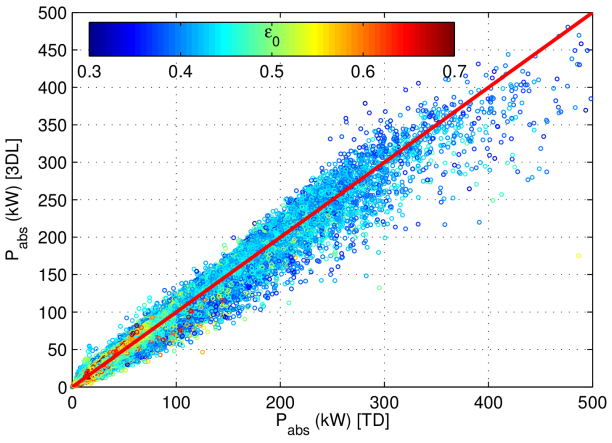

Fig. 4. Scatter plot comparing power performance estimated using the $3DL$ matrix to the 'truth' signal from the time domain model (TD) at Location 1.

TABLE III
MAEP AT LOCATION 1 AS A FUNCTION OF THE NUMBER OF YEAR USED TO CONSTRUCT THE PERFORMANCE MATRIX.

	MAEP (MWH)			% Difference	
Year Range	TD	2DL	3DL	2DL	3DL
2001 - 2001	477.5	495.6	485.3	3.8	1.6
2001 - 2002	486.2	496.8	480.4	2.2	-1.2
2001 - 2003	488.5	499.8	485.1	2.3	-0.7
2001 - 2004	488.2	497.8	483.8	2.0	-0.9
2001 - 2005	486.0	494.8	481.4	1.8	-0.9
2001 - 2006	487.3	491.5	482.3	0.9	-1.0
2001 - 2007	487.5	490.4	484.3	0.6	-0.7
2001 - 2008	487.6	489.9	483.3	0.5	-0.9
2001 - 2009	487.9	489.8	483.9	0.4	-0.8
2001 - 2010	488.1	490.7	485.4	0.5	-0.6
2001 - 2011	488.2	490.5	485.1	0.5	-0.6
2001 - 2012	488.3	490.3	485.2	0.4	-0.6
2001 - 2013	488.3	490.9	485.9	0.5	-0.5

The factors that contribute to the variability of L within each bin (here primarily variations in spectral shape) are quickly averaged out to yield a reasonable estimate of the long-term mean. So even though there is significant scatter when the time-series of records are compared, the objective results, MAEP, converges to the 'true' value.

B. Analysis at Location 2

1) Time-series: In this Section we examine the accuracy achieved using the performance matrices generated for Location 1 to estimate performance at Location 2. As in Section IV-A1, here we use the $2DL$ and $3DL$ matrices generated from the complete 13 years of time domain simulations at Location 1 (see Fig. 2 for $2DL$).

The $2DL$ and $3DL$ were interpolated using the met-ocean data from Location 2 to estimate of the mean P_{abs} record. This estimated record is compared to the 'truth' signal generated with the time domain model. Figs. 6 and 7 show the scatter plots comparing the 'true' P_{abs} with the P_{abs} estimated by interpolation of the $2DL$ and $3DL$ matrices respectively. The colours in the scatter indicate the value of ϵ_0.

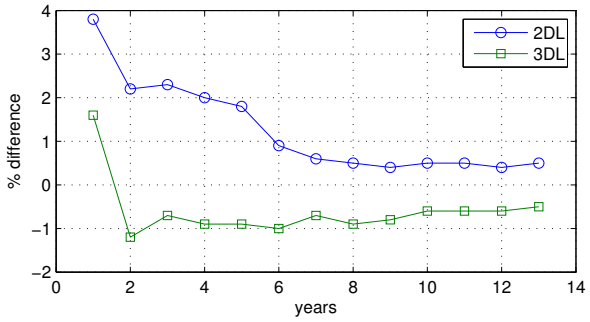

Fig. 5. Difference in MAEP between 'truth' signal and $2DL$ and $3DL$ estimates as a function of the duration of the performance data set at Location 1.

Figure 6 indicates a similar ϵ_0 dependant bias in $2DL$ based estimates of P_{abs} to that observed at Location 1. The $3DL$ based estimates of P_{abs} shown in Fig. 7 show that the ϵ_0 dependant bias in P_{abs} is significantly reduced compared to the $2DL$ estimates, but not eliminated.

A Location 2 there is a are significant occurrences of energetic narrow banded sea-states with $\epsilon_0 < 0.2$. These sea states generally correspond to developing, moderately energetic local wind seas. At Location 1 such conditions with $\epsilon_0 < 0.2$ occur very infrequently. In the $2DL$ matrix this means that the mean L values in each bin are dominated by wider band-width seas which occur more frequently at Location 1. In the $3DL$ matrix it means that most of the bins in the $\epsilon_0 < 0.2$ range contain only one or two records. One or two records are insufficient to achieve a representative bin mean value. These inaccurate bins are the reason for the reason that the P_{abs} bias is not more significantly reduced in the $3DL$ estimates.

It should also be highlighted that the maximum values (P>300kW) are clearly underestimated with the 2D approach. This issue improves with the 3D estimation as most of these points get closer to the real value, and the the underestimation is relatively compensated.

Overall the P_{abs} time-series estimated using the $2DL$ matrix is reasonable; the bias, rms error and correlation coefficient are: -4.5kW, 10.5kW, 97%. Using the $3DL$ matrix improves the bias, rms error and correlation coefficient to: -2.1kW, 9.1kW and 97%.

2) MAEP: Here we investigate the length of the data-set needed to generate a performance matrix which yields accurate MAEP estimates at Location 2. Where Section IV-B1 used all 14 years of available performance data to produce the 2D and 3D matrices, here we repeat that procedure using 1,2,3...14 years of performance data.

Some of the bins in the $2DL$ and $3DL$ matrices are

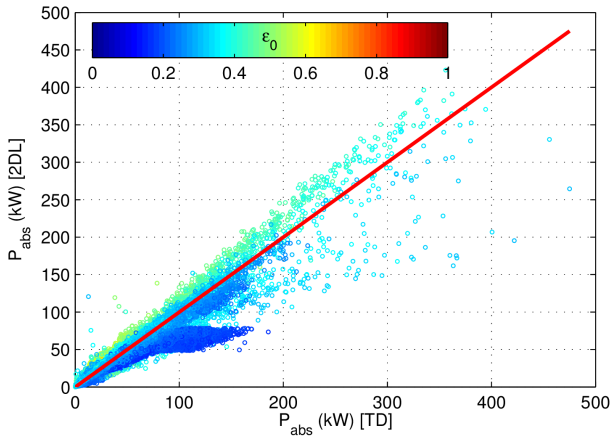

Fig. 6. Scatter plot comparing power performance estimated using the 2D L matrix to the 'truth' signal from the time domain model (TD) at Location 2.

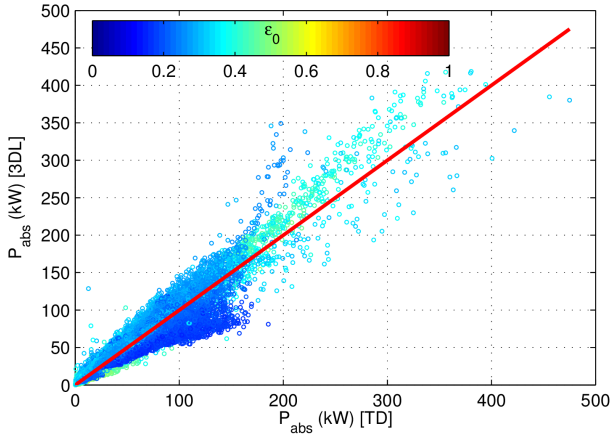

Fig. 7. Scatter plot comparing power performance estimated using the 3D L matrix to the 'truth' signal from the time domain model (TD) at Location 2.

undefined because there were no sea-state occurrences which fell into that bin at Location 1 (e.g. blank cells in Fig. 2). This can result in invalid estimates of L when the matrices are interpolated with met-ocean data from Location 2. In this analysis we compare only those records where the $2DL$, $3DL$ and TD data are valid. This may result in a biased estimate of the absolute MEAP, but enables direct comparison of the MEAP estimated by each method.

Table IV compares the 'true' MAEP calculated with the time domain model to the MAEP estimated from the Location 1 $2DL$ and $3DL$ matrices as a function of the length of the performance data set. In this case, for a short length of the available data the $3DL$ matrix improves the MAEP estimation by 10 to 15% compared to the $2DL$ matrix.

Both the $2DL$ and $3DL$ based estimates of MAEP improve only slightly with the data length. This likely occurs because neither the $2DL$ or $3DL$ matrices completely capture the performance variability of the WEC. The WEC is sensitive to aspects of spectral shape which are not captured by H_{m0},

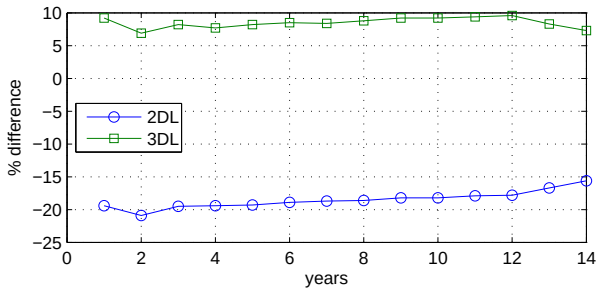

Fig. 8. Difference in MAEP between 'truth' signal and 2Dl and 3DL estimates as a function of the duration of the performance data set at Location 2.

T_e and ϵ_0. As a result, the mean value of L in each bin of the performance matrices from Location 1 converge to a value that is specific to the prevailing wave conditions at Location 1. If the prevailing wave conditions at Location 2 are different, then the mean value of L in each bin will also be slightly different.

To explore this issue further, $2DL$ or $3DL$ matrices were created using the time domain simulation results from Location 2. These were then compared to the performance matrices generated for Location 1. Figure. 9 shows the percentage difference in the $2DL$ matrices for the full duration data-sets from Location 1 and Location 2. From this plot it is evident that the $2DL$ matrix from Location 1 tends to under-estimate L for short period waves and over estimate L for longer period waves. The rms percentage difference in the $2DL$ matrix is 30%, while the rms difference in the $3DL$ matrix is 23%, illustrating that increased dimensionality reduces the uncertainty in each bin.

This analysis shows that additional dimensions in the performance matrix may be required when using performance data from one location to estimate performance at another. By adding additional dimensions to the performance matrix, the performance variability within each bin will be reduced and the mean L will converge towards a 'true' value which is invariant of location.

It should be noted that the level of error in the estimate of the performance matrix developed at Location 1 for application at Location 2 will be dependant on the similarities in the wave climates at the two locations. In this case we intentionally selected two locations with different prevailing wave conditions so that the benefits of increased dimensionality of the performance matrix could be illustrated. Where both locations are subject to similar prevailing wave conditions, a lower dimensionality performance matrix may be sufficient.

V. Conclusions

In this case study, example power performance assessments using the IEC/TS-62600-100 and IEC/TS-62600-102 specified methodologies were performed for using time domain model simulations of a two body self reacting point absorber at two locations in Canada: one off the Atlantic coast and one off the Pacific coast. These examples were used to study the

TABLE IV
MAEP AT LOCATION 2 AS A FUNCTION OF THE NUMBER OF YEAR USED TO CONSTRUCT THE PERFORMANCE MATRIX.

	MAEP (MWH)			% Difference	
Year Range	TD	2DL	3DL	2DL	3DL
1988 - 1988	251.3	202.6	274.4	-19.4	9.2
1988 - 1989	241.9	191.5	258.5	-20.9	6.9
1988 - 1990	231.5	186.5	250.5	-19.5	8.2
1988 - 1991	235.2	189.5	253.3	-19.4	7.7
1988 - 1992	233.0	188.2	252.1	-19.3	8.2
1988 - 1993	232.7	188.8	252.5	-18.9	8.5
1988 - 1994	234.3	190.4	253.9	-18.7	8.4
1988 - 1995	234.7	191.1	255.3	-18.6	8.8
1988 - 1996	235.9	193.0	257.7	-18.2	9.2
1988 - 1997	240.4	196.6	262.5	-18.2	9.2
1988 - 1998	242.0	198.6	264.8	-17.9	9.4
1988 - 1999	243.2	200.0	266.7	-17.8	9.6
1988 - 2000	250.8	208.9	271.5	-16.7	8.3
1988 - 2001	250.2	211.1	268.4	-15.6	7.3

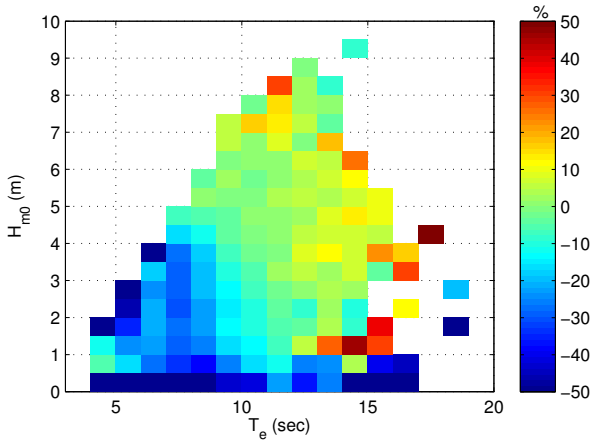

Fig. 9. Percentage difference in $2DL$ matrices calculated from time domain simulations at Location 1 and Location 2.

influence of the dimensionality of the performance matrix and the duration of the performance data series on power performance estimates

Performance matrices were constructed using both the traditional 2D (H_{m0}-T_e) approach, and a 3D approach where the additional dimension is spectral band width. The influence of dimensionality was investigated by comparing the performance estimates using the 2D and 3D matrices to the time domain model results. In the IEC/TS-62600-100 analysis, the 3D performance matrix approach was shown to reduce the bias and scatter and increase correlation in the performance estimates. Similar results were found in the IEC/TS-62600-102 analysis, however, not to the extent observed in the IEC/TS-62600-100 analysis. The difference in the efficacy of the 3D performance matrix is due differences in the wave climate between locations which are not captured by H_{m0}, T_e and e_0.

The duration of the performance data series used to generate both the performance matrices was varied at 1 year increments up to the maximum duration of the performance data series (13 and 14 years). The influence of the data series duration was investigated by comparing the mean annual energy production estimated using the performance matrices and calculated using the time domain model. In the IEC/TS-62600-100 analysis, for a short data series, it was found that the 3D matrix improves estimate accuracy by 2 to 3 % compared to the 2D matrix. For long data series both methods approach the same accuracy; though the 2D method requires 6 years to reach a 1% error level, while the 3D method requires only 2. In the IEC/TS-62600-102 analysis, for a short data series, it was found that the 3D matrix improves estimate accuracy by 10 to 15 % compared to the 2D matrix. However, both the 2D and 3D estimates improve minimally with data series duration.

The results presented here illustrate that additional dimensions in the performance matrix may be required when using data from one location to estimate performance at another. By adding additional dimensions to the performance matrix, the performance variability within each bin will be reduced and the mean performance will converge towards a value which is invariant of location.

ACKNOWLEDGMENT

The authors gratefully acknowledge the support from Marine Renewables Canada, Canadian Sub-Committee to the IEC TC114, Pacific Institute for Climate Solutions (PICS), Natural Resources Canada (NRCan), Natural Sciences and Engineering Research Council (NSERC) of Canada. The authors would also like to acknowledge to the DTOcean project, funded by the European Commission with Grant Agreement number 608597 for allowing Adrian to work on this collaborative work.

REFERENCES

[1] *IEC/TS 62600-100 ed1.0: Power Performance Assessment of Electricity Producing Wave Energy Converters*, TC114 Std.

[2] M.-A. Kerbiriou, M. Prevosto, C. Maisondieu, A.Clement, and A.Babarit, "Influence of an improved sea-state description on a wave energy converter production," in *the 26th International Conference on Offshore Mechanics and Arctic Engineering*, 2007.

[3] ——, "Influence of sea-states description on wave energy production assessment," in *The 7th European Wave and Tidal Energy Conference, Porto, Portugal*, 2007.

[4] J.-B. Saulnier, A. Clment, A. F. d. O. Falco, T. Pontes, M. Prevosto, and P. Ricci, "Wave groupiness and spectral bandwidth as relevant parameters for the performance assessment of wave energy converters," *Ocean Engineering*, vol. 38, no. 1, pp. 130–147, Jan. 2011. [Online]. Available: http://www.sciencedirect.com/science/article/pii/S0029801810002179

[5] J.-B. Saulnier, M. Prevosto, and C. Maisondieu, "Refinements of sea state statistics for marine renewables: A case study from simultaneous buoy measurements in portugal," *Renewable Energy*, vol. 36, no. 11, pp. 2853–2865, Nov. 2011. [Online]. Available: http://www.sciencedirect.com/science/article/pii/S096014811100187X

[6] D. Clabby, A. Henry, M. Folley, and T. Whittaker, "The effect of the spectral distribution of wave energy on the performance of a bottom hinged flap type wave energy converter," in *ASME 2012 31st International Conference on Ocean, Offshore and Arctic Engineering*, 2012.

[7] R. Pascal, G. Payne, C. Theobald, and I. Bryden, "Parametric models for the performance of wave energy converters*," *Applied Ocean Research*, vol. 38, no. 0, pp. 112–124, Oct. 2012. [Online]. Available: http://www.sciencedirect.com/science/article/pii/S0141118712000533

[8] A. de Andrs, R. Guanche, J. Armesto, F. del Jesus, C. Vidal, and I. Losada, "Time domain model for a two-body heave converter: Model and applications," *Ocean Engineering*, vol. 72, no. 0, pp. 116–123, Nov. 2013. [Online]. Available: http://www.sciencedirect.com/science/article/pii/S0029801813002655

[9] A. de Andres, R. Guanche, J. Weber, and R. Costello, "Finding gaps on power production assessment on wecs: wave definition analysis," *Renewable Energy*, 2015, under review- RENE-D-14-01260.

[10] S. Beatty, M. Hall, B. Buckham, and P. Wild, "Experimental comparison of self-reacting point absorber wec designs," in *the 10th European Wave and Tidal Conference*, 2013.

[11] Department of Fisheries and Oceans, Canada, "Oceanography and scientific data," March 2015. [Online]. Available: http://www.meds-sdmm.dfo-mpo.gc.ca/isdm-gdsi/waves-vagues/index-eng.htm

[12] D. W. Wang and P. A. Hwang, "An operational method for separating wind sea and swell from ocean wave spectra*," *J. Atmos. Oceanic Technol.*, vol. 18, no. 12, pp. 2052–2062, Dec. 2001. [Online]. Available: http://dx.doi.org/10.1175/1520-0426(2001)018⟨2052:AOMFSW⟩2.0.CO;2

[13] W. Cummins, "The impulse response function and ship motions," David Taylor Model Basin, Department of the Navy, Tech. Rep., 1962.

[14] DNV, "Recommended practice DNV-RP-C205 environmental conditions and environmental loads," Det Norske Veritas, 2010.